This article has been accepted for publication in a future issue of this journal, but has not been fully edited. Content may change prior to final publication. Citation information: DOI 10.1109/JIOT.2018.2792300, IEEE Internet of Things Journal

Optimization Algorithms for Multi-Access Green Communications in Internet of Things

Xiangping (Bryce) Zhai, *Member, IEEE*, Xiaoxiao Guan, Chunsheng Zhu, *Member, IEEE*, Lei Shu, *Senior Member, IEEE*, and Jiabin Yuan

***Abstract*—The exponential increase of the intelligent connected devices and the dramatic growth of the wireless data traffic have motivated the development of the green wireless networks as well as the Internet of Things. In this paper, we study the minimization problem of the total power to satisfy the required rate constraints in Internet of Things, where the users simultaneously communicate through multiple independent channels. This problem is complicated due to the non-linear data rate function based on the Shannon capacity formula. To this end, we first transfer the initial problem in power domain to an equivalent problem in rate domain instead of direct approximation for the high data rate. Then, we approximate it to a convex problem with the spectral radius constraints by the use of the Neumann expansion and nonlinear Perron-Frobenius theorem. By doing so, we achieve the close upper bound for this total power minimization problem. Moreover, we obtain the lower bound by making use of the convex relaxation technique, and finally get the global optimal solution by leveraging the branch-and-bound method. Simulation results verify that our proposed algorithms have a good approximation to the global optimal value for the power and rate allocations.**

***Index Terms*—Internet of Things, green communications, multi-access management, convex approximation, nonnegative matrix theory.**

I. Introduction

In recent years, various successful demonstrations of the mobile technologies for the wireless communications have been witnessed. Since its first generation in the last 1970s, the mobile services have come across from the analog system, digital system, internet system to the current worldwide constructed integration system, which is adept at providing high quality mobile broadband services to guarantee the high data rates [1]. Over the last couple of years, the Internet has been in a constant state of evolution and the next generation mobile communication is envisioned to be available after 2020. As a part of this development, 5G and the Internet of Things (IoT) with some emerging technologies are regarded as a new round of industrial and technological revolution after the steam, electric, computer and Internet [2], [3]. IoT is expected to possess important home and business meanings based on the evolution of the sensor networks, to achieve more intelligent applications for the contributions to the quality of life and the global economy [4], [5].

Nowadays, the wireless communications become more efficient in the aspects of the practice and appearance, as the dual standby mode technique enable that the users automatically search networks and switch between them within a tiny moment. Multi-access is useful for the practical applications [6]. However, the utilization and conservation of resources turn into the major issue when the mobile users take the rapid authentication and fast switch between different independent channels [7], with the fact that the mobile users can only use a single channel at a time. Therefore, we aim at the system in which the mobile users simultaneously access several available

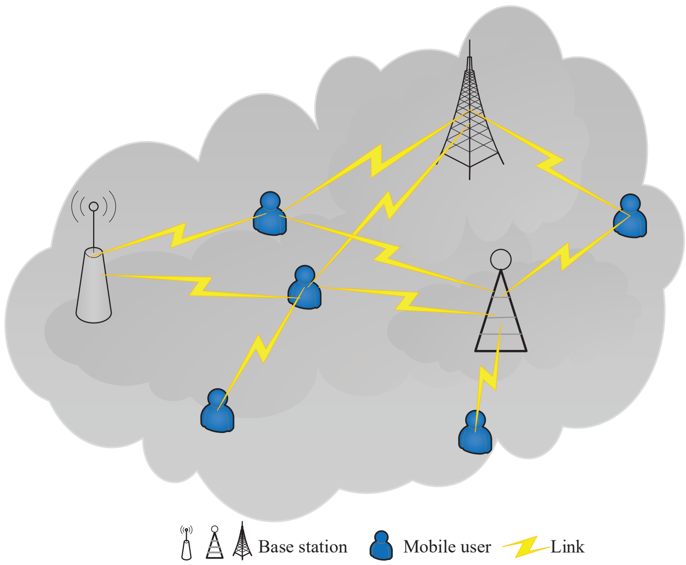

Fig. 1: An illustration of the wireless network where the users transmit information through one or more channels, simultaneously.

X. Zhai, X. Guan and J. Yuan are with the College of Computer Science and Technology, Nanjing University of Aeronautics and Astronautics, Nanjing 211106, China, and also with the Collaborative Innovation Center of Novel Software Technology and Industrialization, Nanjing 210032, China (e-mail: blueicezhaixp@nuaa.edu.cn; gxiaoxiao@nuaa.edu.cn; ok@nuaa.edu.cn).

C. Zhu is the corresponding author with the Department of Electrical and Computer Engineering, University of British Columbia, Vancouver, BC V6T 1Z4, Canada (e-mail: cszhu@ece.ubc.ca).

L. Shu is with NAU-Lincoln Joint Research Center of Intelligent Engineering, Nanjing Agricultural University, China, 210000 and with School of Engineering in College of Science, University of Lincoln, UK, INB3235, Engineering Hub, Brayford Pool, Lincoln, LN67TS, United Kingdom (e-mail: lei.shu@ieee.org).

This work was supported in part by National Natural Science Foundation of China under Grant No. 61701231, in part by International and Hong Kong, Macao, and Taiwan collaborative innovation platforms, by major international cooperation projects of colleges in Guangdong Province under Grant No. 2015KGJHZ026, and in part by Maoming Engineering Research Center of Industrial Internet of Things under Grant No. 517018. The material in this paper was presented in part at the 18th IEEE International Conference on High Performance Computing and Communications, Sydney, Australia, 2016.

This article has been accepted for publication in a future issue of this journal, but has not been fully edited. Content may change prior to final publication. Citation information: DOI 10.1109/JIOT.2018.2792300, IEEE Internet of Things Journal

channels based on multiple SIM-cards so as to reduce the waste of channel resources and to guarantee the high data rates in this paper. We consider that the multi-users share the multi-channels in IoT to improve the channel utilization. Each mobile user simultaneously transmits information via different channels to achieve its rate requirement. Figure 1 illustrates an example of our considered networks.

The network expansion has posed serious challenges with respect to energy consumption. It is the general trend of development towards the green wireless communications with the rapid growth of the intelligent terminals for the future wireless networks design [8], [9]. Typically, the power control is an effective approach for supporting the high performance while decreasing the energy cost [10], [11]. In [12], the authors investigated the total power minimization problem in a NOMA-based heterogeneous network under 5G by an iterative algorithm. In [13], the authors addressed the power consumption minimization in an OFDM-based heterogeneous network through an efficient iterative algorithm for sub-channel assignment and power distribution. Moreover, the authors tackled the total power minimization problem in the cellular system with underlaying Device-to-Device (D2D) communications in [14]. From the perspective of the end user, the issue of improving energy efficiency is then brought into playing for the sake of extending battery life. Even if a break-through happened in the battery technology, the environment and society responsibility would still trigger the high energy efficiency. The authors in [15] explored the resource and power optimization to maximize the energy efficiency of Device-to-Device communications in the underlaying cellular networks. The authors in [16] studied the energy-efficient QoS-aware resource allocation problem in the heterogeneous OFDM-based networks by dual decomposition method. Besides, the authors in [17] devised the global optimal power allocation and antenna selection algorithm by using the mixed-integer nonlinear programming and the branch-and-bound method. Last but not least, there are many works has great interests in the context of enhancing the system throughput towards the higher-performance of the network. The branch-and-bound framework is usually adopted to give the optimal solution for the small scale NP-hard problem, e.g., the throughput optimization problem under the ratio of the received signal power to the additive noise and sum of interference signal power (SINR) model in [18]. The authors in [19] maximized the weighted sum rate problem with both interference temperature constraints and power budgets by the reformulation-relaxation technique. Including the listed works above, most existing researches are absorbed in the wireless networks with single channel. However, wireless networks with multi-channels gain an advantage owing to the scarcity of the spectrum resources. The authors in [20] used the game theory to study the downlink transmission in a wireless cellular relay network with multi-users and multi-channels. The authors in [21] investigated the throughput maximization in cognitive radio networks with multi-channels using the cooperative sensing.

Motivated by the aforementioned reviews, we study a total power minimization problem in IoT with multi-access communications to improve the resource utilization with minimal energy consumption in this paper. The optimization problem is formulated with the individual rate and power constraints, which is a non-linear optimization problem and thus is difficult to tackle. Though we can directly approximate the high rate function in power domain, we provide the closer upper bound for this total power minimization problem by approximating it to a convex problem in rate domain. Then, we exploit the convex relaxation to find the lower bound [22]. Furthermore, we get the global optimal value by leveraging the branch-and-bound method. Some key techniques in the nonnegative matrix theory like subinvariance theorem, Perron-Frobenius theorem and quasi-invertibility are employed in our paper. In sum, the main contributions in this paper are listed as follows:

1) We study the total power minimization problem with rate constraints and transfer it to the rate domain from the power domain by utilizing the reformulation technique, as there is an one-to-one mapping relationship between the power and rate.
2) Based on the nonnegative matrix theory, we convexify the non-convex problem for the total energy minimization by the aid of the spectral radius constraints. Then, we get the upper bound through the convex approximation algorithm.
3) According to the convex relaxation technique and the branch-and-bound framework, we compare our approximation to the global optimal value obtained by the proposed global optimization algorithm adopting the convex approximation algorithm as the inner loop.

The rest parts are organized as follows: We describe the system model and formulate the total power minimization problem in Section II. In Section III, we transfer the problem to the rate domain from the power domain for the algorithm design. In Section IV, we obtain the approximate value by convexifying the total power minimization problem, which can be used as the upper bound. Furthermore, we propose a global optimal algorithm in Section V for comparison. In Section VI, the simulation results numerically evaluated our algorithms, with the conclusion followed in Section VII.

Notations: The Perron-Frobenius eigenvalue, i.e., the spectral radius, is denoted by $\rho(\cdot)$. The transpose is denoted by the super-script $(\cdot)^\top$. We denote $\mathbf{I}$ as the identity matrix, $\mathbf{1}$ as $(1, \cdots, 1)^\top$, and $\mathbf{e}_l$ as the l-th unit coordinate vector, respectively. In addition, $\mathrm{diag}(\mathbf{x})$ denotes the diagonal matrix with the entries of $\mathbf{x}$ on the diagonal, for the vector $\mathbf{x} = (x_1, \cdots, x_n)^\top$. Let $e^{\mathbf{x}}$ denote $(e^{x_1}, \cdots, e^{x_n})^\top$ and $\log \mathbf{x}$ denote $(\log x_1, \cdots, \log x_n)^\top$, respectively.

II. System Model

There are finite mobile users and independent channels in the system networks, while the mobile users simultaneously access a series of different channels. Let M and L denote the number of channels and mobile users in all, respectively. Assuming that the same common frequency-flat fading channel is shared by the users when they transmit through the same channel, and each user has excellent channel state information at its receiver. We use superscript m to index the channels and subscript l to index the mobile users, respectively. Then, we

This article has been accepted for publication in a future issue of this journal, but has not been fully edited. Content may change prior to final publication. Citation information: DOI 10.1109/JIOT.2018.2792300, IEEE Internet of Things Journal

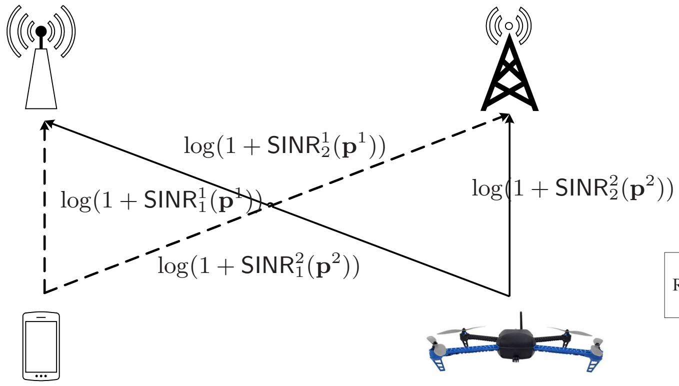

Fig. 2: A two-user example illustration with two mobile network operators having independent channels.

have $l \in \mathcal{L}$ with $\mathcal{L} = \{l \mid l = 1, \cdots, L\}$, and $m \in \mathcal{M}$ with $\mathcal{M} = \{m \mid m = 1, \cdots, M\}$. The vector $\mathbf{p}^m = (p_1^m, \cdots, p_L^m)^\top$ denotes the transmit power vector in the m-th channel. The additive white Gaussian noise is regarded as the interference. The vector $\boldsymbol{\sigma}^m = (\sigma_1^m, \cdots, \sigma_L^m)^\top$ represents the noise power vector, where σ_l^m denotes the noise power of the l-th user in the m-th channel. Let the SINR of the l-th user in the m-th channel be written in terms of $\mathbf{p}^m$ as:

$$\mathsf{SINR}_l^m(\mathbf{p}^m) = \frac{G_{ll}^m p_l^m}{\sum_{j \neq l} G_{lj}^m p_j^m + \sigma_l^m}, \tag{1}$$

where G_{lj}^m is denoted as the channel gain at the l-th receiver from the j-th transmitter in the m-th channel. $\mathbf{G}^m$ is the corresponding channel gain matrix with the entries of G_{lj}^m. Based on the Shannon capacity formula, the data rate of the l-th user in the m-th channel is given by:

$$\log\left(1 + \mathsf{SINR}_l^m(\mathbf{p}^m)\right). \tag{2}$$

Then, the total power minimization problem for green communications is formulated as follows:

$$\begin{aligned}
&\text{minimize} && \sum_{l=1}^{L} \sum_{m=1}^{M} p_l^m \\
&\text{subject to} && \sum_{m=1}^{M} \log\left(1 + \mathsf{SINR}_l^m(\mathbf{p}^m)\right) \geq \bar{r}_l, \\
& && \quad l = 1, \cdots, L;\ m = 1, \cdots, M, \\
& && p_l^m \leq \bar{p}_l^m,\ l = 1, \cdots, L;\ m = 1, \cdots, M, \\
& && \mathbf{p}^m \geq \mathbf{0},\ m = 1, \cdots, M, \\
&\text{variables:} && \mathbf{p}^m,\ m = 1, \cdots, M,
\end{aligned} \tag{3}$$

where $\bar{p}_l^m > 0$ denotes the budget of transmit power for the l-th user in the m-th channel, and $\bar{r}_l$ is positive to denote the data rate requirement of the l-th mobile user in all channels. Figure 2 shows an example of the wireless network with two mobile network operations having independent channels. Given the individual power and rate constraints, the total power minimization problem (3) is a non-convex problem due to the complicated Shannon capacity rate function (2), and thus is difficult to tackle.

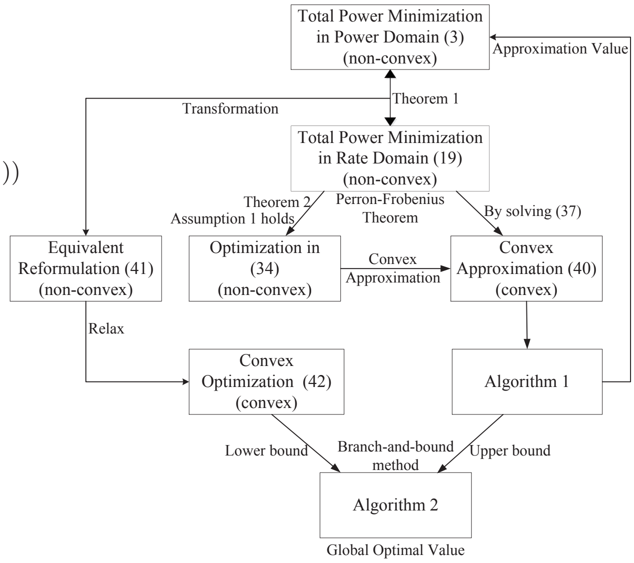

Fig. 3: A summary of the techniques for the total power minimization problem.

For the convenience of the following analyses, we define the nonnegative matrix $\mathbf{F}^m$ with entries as:

$$F_{lj}^m = \begin{cases} 0, & \text{if } l = j \\ G_{lj}^m / G_{ll}^m, & \text{otherwise } l \neq j \end{cases} \tag{4}$$

and the vector $\mathbf{v}$ as:

$$\mathbf{v}^m = \left(\frac{\sigma_1^m}{G_{ll}^m}, \frac{\sigma_2^m}{G_{22}^m}, \cdots, \frac{\sigma_L^m}{G_{LL}^m} \right)^\top. \tag{5}$$

Then, we rewrite (1) as:

$$\mathsf{SINR}_l^m(\mathbf{p}^m) = \frac{p_l^m}{(\mathbf{F}^m \mathbf{p}^m + \mathbf{v}^m)_l}. \tag{6}$$

Figure 3 gives the outline of the main techniques used in this paper. First, we reformulate non-convex (3) in power domain into non-convex (19) in rate domain using Theorem 1. Note that it plays an important part in the algorithm design by using the convex approximation technique. Based on the convex approximation technique and Perron-Frobenius theorem, we obtain the convex problem (40) (cf. Section IV). Then, Algorithm 1 gets the approximation value and provides the upper bound for Algorithm 2. Moreover, we transform (3) into an equivalent (41) and relax (41) to a convex optimization problem (42) to offer the lower bound (cf. Section V). Taking the convex approximation algorithm as the inner loop and employing the branch-and-bound method, Algorithm 2 solves (3) global optimally.

III. Problem Reformulation

In this section, we take a series of transformations to get the one-to-one mapping between $\mathbf{p}^m$ and $\mathbf{r}^m$, and then reformulate (3) from the power domain into the equivalent rate domain. We first introduce the auxiliary variable r_l^m to investigate the following equivalent optimization problem:

$$
\begin{aligned}
\text{minimize} \quad & \sum_{l=1}^{L}\sum_{m=1}^{M} p_l^m \\
\text{subject to} \quad & \log\left(1+\mathsf{SINR}_l^m(\mathbf{p}^m)\right) \ge r_l^m, \\
& \quad l=1,\cdots,L;\ m=1,\cdots,M, \\
& \mathbf{r}^m \ge \mathbf{0},\ m=1,\cdots,M, \\
& \sum_{m=1}^{M} r_l^m \ge \bar{r}_l,\ l=1,\cdots,L, \\
& \mathbf{p}^m \ge \mathbf{0},\ m=1,\cdots,M, \\
& p_l^m \le \bar{p}_l^m,\ l=1,\cdots,L;\ m=1,\cdots,M, \\
\text{variables}: \quad & \mathbf{p}^m,\ \mathbf{r}^m,\ m=1,\cdots,M.
\end{aligned} \tag{7}
$$

Now, (7) is non-convex solely due to the non-convex individual rate constraint, i.e., $\log\left(1+\mathsf{SINR}_l^m(\mathbf{p}^m)\right) \ge r_l^m$. When the rate or the SINR is high, we can approximate $\log\left(1+\mathsf{SINR}_l^m(\mathbf{p}^m)\right)$ by $\log\left(\mathsf{SINR}_l^m(\mathbf{p}^m)\right)$ to get the following convex problem directly [23]:

$$
\begin{aligned}
\text{minimize} \quad & \sum_{l=1}^{L}\sum_{m=1}^{M} p_l^m \\
\text{subject to} \quad & \log\left(\mathsf{SINR}_l^m(\mathbf{p}^m)\right) \ge r_l^m, \\
& \quad l=1,\cdots,L;\ m=1,\cdots,M, \\
& \sum_{m=1}^{M} r_l^m \ge \bar{r}_l,\ l=1,\cdots,L, \\
& p_l^m \le \bar{p}_l^m,\ l=1,\cdots,L;\ m=1,\cdots,M, \\
& \mathbf{p}^m \ge \mathbf{0},\ m=1,\cdots,M, \\
& \mathbf{r}^m \ge \mathbf{0},\ m=1,\cdots,M, \\
\text{variables}: \quad & \mathbf{p}^m,\ \mathbf{r}^m,\ m=1,\cdots,M.
\end{aligned} \tag{8}
$$

The convex problem (8) is a approximation to (7), and thus can be numerically solved by directly using the interior-point solvers, e.g., the cvx software [24]. The experimental results are demonstrated in Section VI. However, we can obtain a closer approximation value by the convex approximation algorithm in Section IV, which is more efficient as the upper bound for our global optimal algorithm in Section V.

Then, we introduce another helpful auxiliary variable $\mathbf{q}^m = \mathbf{F}^m\mathbf{p}^m + \mathbf{v}^m$ for all m-th channels, which is noise plus the total interference and can represent as the interference temperature [25]. Thus, we rewrite (1) into:

$$
\mathsf{SINR}_l^m(\mathbf{p}^m) = \frac{p_l^m}{q_l^m}. \tag{9}
$$

It is noticed that the individual rate constraint is tight at optimality. Then, we obtain the following three important relationships:

$$
\begin{cases}
\mathrm{diag}(e^{\mathbf{r}^m})\mathbf{q}^m = \mathbf{p}^m + \mathbf{q}^m, \\
\mathbf{p}^m = \mathrm{diag}(e^{\mathbf{r}^m}-1)(\mathbf{F}^m\mathbf{p}^m + \mathbf{v}^m), \\
\mathbf{q}^m = \mathbf{F}^m\mathrm{diag}(e^{\mathbf{r}^m}-1)\mathbf{q}^m + \mathbf{v}^m.
\end{cases} \tag{10}
$$

Assuming the matrices $\mathbf{I}-\mathrm{diag}(e^{\mathbf{r}^m}-1)\mathbf{F}^m$ and $\mathbf{I}-\mathbf{F}^m\mathrm{diag}(e^{\mathbf{r}^m}-1)$ are invertible, we obtain two one-to-one mappings in terms of $\mathbf{r}^m$, respectively:

$$
\mathbf{p}^m(\mathbf{r}^m) = \Big(\mathbf{I}-\mathrm{diag}(e^{\mathbf{r}^m}-1)\mathbf{F}^m\Big)^{-1}\mathrm{diag}(e^{\mathbf{r}^m}-1)\mathbf{v}^m, \tag{11}
$$

and:

$$
\mathbf{q}^m(\mathbf{r}^m) = \Big(\mathbf{I}-\mathbf{F}^m\mathrm{diag}(e^{\mathbf{r}^m}-1)\Big)^{-1}\mathbf{v}^m. \tag{12}
$$

Next, we study a equivalent reparameterization of (3), which has only the introduced rate variable $\mathbf{r}^m$ to be optimized.

Theorem 1. *The linear system in terms of $\boldsymbol{p}^m$:*

$$
\begin{cases}
\boldsymbol{p}^m = \mathrm{diag}(e^{\mathbf{r}^m}-1)\boldsymbol{F}^m\boldsymbol{p}^m + \mathrm{diag}(e^{\mathbf{r}^m}-1)\boldsymbol{v}^m, \\
\mathbf{0} \le \boldsymbol{p}^m \le \bar{\boldsymbol{p}}^m,
\end{cases} \tag{13}
$$

for each m-th channel, has a feasible solution, if and only if:

$$
\rho\left(\mathrm{diag}(e^{\mathbf{r}^m}-1)\left(\boldsymbol{F}^m + \frac{1}{\bar{p}_l^m}\boldsymbol{v}^m\boldsymbol{e}_l^\top\right)\right) \le 1. \tag{14}
$$

Proof: Substituting (6) into (2), we obtain:

$$
\mathrm{diag}(e^{\mathbf{r}^m}-1)(\mathbf{F}^m\mathbf{p}^m + \mathbf{v}^m) = \mathbf{p}^m. \tag{15}
$$

From the constraint $p_l^m \le \bar{p}_l^m$ for all l and m, we get $\frac{p_l^m}{\bar{p}_l^m} \le 1$. Then, we have $\frac{1}{\bar{p}_l^m}\mathbf{e}_l^\top\mathbf{p}^m \le 1$ and $\frac{1}{\bar{p}_l^m}\mathbf{v}^m\mathbf{e}_l^\top\mathbf{p}^m \le \mathbf{v}^m$ further. In all, we obtain:

$$
\mathrm{diag}(e^{\mathbf{r}^m}-1)\left(\mathbf{F}^m + \frac{1}{\bar{p}_l^m}\mathbf{v}^m\mathbf{e}_l^\top\right)\mathbf{p}^m \le \mathbf{p}^m. \tag{16}
$$

Now, we state the *Subinvariance Theorem* [26].

Lemma 1. *Let $\boldsymbol{A}$ be a nonnegative irreducible matrix, and Λ be a positive number. $\boldsymbol{v}$ is a nonnegative vector with $\boldsymbol{A}\boldsymbol{v} \le \Lambda\boldsymbol{v}$. Then $\Lambda > \rho(\mathbf{A})$ and $\mathbf{v} > \mathbf{0}$. In addition, $\boldsymbol{A}\boldsymbol{v} = \Lambda\boldsymbol{v}$ if and only if $\Lambda = \rho(\boldsymbol{A})$.*

Let $\Lambda = 1, \mathbf{v} = \mathbf{p}^m$, and $\mathbf{A} = \mathrm{diag}(e^{\mathbf{r}^m} - 1)\left(\mathbf{F}^m + \frac{1}{\bar{p}_l^m}\mathbf{v}^m\mathbf{e}_l^\top\right)$, respectively. We finally obtain (14) by transferring (16) further. This algebraic transformation changes the inequality to be a spectral radius constraint, which motivates us to convexify it [27]. ■

We define the feasible sets:

$$
\mathcal{R}_1 = \left\{ r_l^m \,|\, \sum_{m=1}^{M} r_l^m \ge \bar{r}_l, r_l^m \ge 0 \right\}, \tag{17}
$$

and:

$$
\mathcal{R}_2 = \left\{ r_l^m | \rho\left(\mathrm{diag}(e^{\mathbf{r}^m}-1)\left(\mathbf{F}^m + \frac{1}{\bar{p}_l^m}\mathbf{v}^m\mathbf{e}_l^\top\right)\right) \le 1 \right\}, \tag{18}
$$

according to the statements above.

Finally, we transfer the original problem (3) to the rate domain from the power domain:

$$
\begin{aligned}
\text{minimize} \quad & \sum_{m=1}^{M} f^m(\mathbf{r}^m) \\
\text{subject to} \quad & \mathbf{r}^m \in \mathcal{R}_1 \cap \mathcal{R}_2,\ m=1,\cdots,M, \\
\text{variables}: \quad & \mathbf{r}^m,\ m=1,\cdots,M,
\end{aligned} \tag{19}
$$

This article has been accepted for publication in a future issue of this journal, but has not been fully edited. Content may change prior to final publication. Citation information: DOI 10.1109/JIOT.2018.2792300, IEEE Internet of Things Journal

where $\mathbf{r}^m$ is the only variable, and the objective function in (19) is defined as the mapping in (11), i.e.:

$$f^m(\mathbf{r}^m) = \mathbf{1}^\top \left(\mathbf{I} - \mathrm{diag}(e^{\mathbf{r}^m} - 1)\mathbf{F}^m\right)^{-1} \mathrm{diag}(e^{\mathbf{r}^m} - 1)\mathbf{v}^m. \tag{20}$$

Moreover, we have:

$$\left(\mathbf{I} - \mathrm{diag}(e^{\mathbf{r}^m} - 1)\mathbf{F}^m\right)^{-1} = \sum_{k=0}^{\infty} \left(\mathrm{diag}(e^{\mathbf{r}^m} - 1)\mathbf{F}^m\right)^k, \tag{21}$$

based on Neumann's expansion [28]. We then rewrite (20) as:

$$f^m(\mathbf{r}^m) = \mathbf{1}^\top \left(\sum_{k=1}^{\infty} \left(\mathrm{diag}(e^{\mathbf{r}^m} - 1)\mathbf{F}^m\right)^k\right) (\mathbf{F}^m)^{-1}\mathbf{v}^m. \tag{22}$$

(3) and (19) are equivalent to each other through a series of reformulations above. Both of them are difficult to solve, and the solutions to them are connected by (11). Note that (19) is equivalent to (8) if we approximate $e^{\mathbf{r}^m} - 1$ as $e^{\mathbf{r}^m}$. However, we get the closer approximation by separately tackling $e^{\mathbf{r}^m} - 1$ in the objective function and the spectral radius constraint in the following.

IV. Efficient Convex Approximation Algorithm

We propose an efficient convex approximation algorithm for (19) in this section,. Based on (10), we have:

$$\mathbf{p}^m = \mathrm{diag}(e^{\mathbf{r}^m} - 1)\mathbf{q}^m. \tag{23}$$

Thus, we have another theorem.

Theorem 2. *The linear system in terms of $\boldsymbol{p}^m$ for each m-th channel:*

$$\begin{cases} \boldsymbol{p}^m = \mathrm{diag}(e^{\mathbf{r}^m} - 1)\boldsymbol{F}^m\boldsymbol{p}^m + \mathrm{diag}(e^{\mathbf{r}^m} - 1)\boldsymbol{v}^m, \\ \mathbf{0} \le \boldsymbol{p}^m \le \bar{\boldsymbol{p}}^m, \end{cases} \tag{24}$$

has a feasible solution, if and only if:

$$\begin{aligned} &\left(\boldsymbol{I} + \boldsymbol{F}^m + \frac{1}{\bar{p}_l^m}\mathbf{v}^m\boldsymbol{e}_l^\top\right)\boldsymbol{q}^m \\ \ge\ &\left(\boldsymbol{F}^m + \frac{1}{\bar{p}_l^m}\mathbf{v}^m\boldsymbol{e}_l^\top\right)\mathrm{diag}\left(e^{\mathbf{r}^m}\right)\boldsymbol{q}^m. \end{aligned} \tag{25}$$

Proof: (24) is equivalent to:

$$\mathrm{diag}(e^{\mathbf{r}^m} - 1)\left(\mathbf{F}^m + \frac{1}{\bar{p}_l^m}\mathbf{v}^m\mathbf{e}_l^\top\right)\mathbf{p}^m \le \mathbf{p}^m, \tag{26}$$

based on Theorem 1. Substituting (23) into (26), we obtain:

$$\begin{aligned} &\mathrm{diag}(e^{\mathbf{r}^m} - 1)\left(\mathbf{F}^m + \frac{1}{\bar{p}_l^m}\mathbf{v}^m\mathbf{e}_l^\top\right)\mathrm{diag}(e^{\mathbf{r}^m} - 1)\mathbf{q}^m \\ \le\ &\mathrm{diag}(e^{\mathbf{r}^m} - 1)\mathbf{q}^m. \end{aligned} \tag{27}$$

Since $\mathbf{r}^m \ge \mathbf{0}$ for $m \in \mathcal{M}$, we have:

$$\left(\mathbf{F}^m + \frac{1}{\bar{p}_l^m}\mathbf{v}^m\mathbf{e}_l^\top\right)\mathrm{diag}(e^{\mathbf{r}^m} - 1)\mathbf{q}^m \le \mathbf{q}^m. \tag{28}$$

Then, the feasible condition is proved. ■

Theorem 2 motivates us to convexify (19) to a convex set, which can be then addressed in polynomial time by the interior point method. Then, we make the convex approximation by using the assumption and the reformulation-approximation technique in [19]. We propose the efficient convex approximation algorithm to compute an approximation value which provides the efficient upper bound for Algorithm 2 in Section V.

A. Special Instance

Assumption 1. *Define the matrix $\mathbf{B}_l^m$:*

$$\boldsymbol{B}_l^m = \boldsymbol{F}^m + \frac{1}{\bar{p}_l^m}\mathbf{v}^m\boldsymbol{e}_l^\top. \tag{29}$$

Then, the following is satisfied:

$$\widetilde{\boldsymbol{B}}_l^m = (\boldsymbol{I} + \boldsymbol{B}_l^m)^{-1}\boldsymbol{B}_l^m \ge 0,\ m \in \mathcal{M},\ l \in \mathcal{L}, \tag{30}$$

where $\widetilde{\boldsymbol{B}}_l^m$ is an irreducible nonnegative matrix and $\boldsymbol{B}_l^m$ is a nonnegative matrix.

Note that this assumption means that the matrix $\widetilde{\mathbf{B}}_l^m$ is also a nonnegative matrix, when there is a nonnegative matrix $\mathbf{B}_l^m$. We rewrite (19) into the following matrix form:

$$\begin{aligned} \text{minimize}\quad & \sum_{m=1}^{M} \mathbf{1}^\top\left(\sum_{k=1}^{\infty}\left(\mathrm{diag}(e^{\mathbf{r}^m} - 1)\mathbf{F}^m\right)^k\right)(\mathbf{F}^m)^{-1}\mathbf{v}^m \\ \text{subject to}\quad & \mathbf{r}^m \ge \mathbf{0},\ m = 1, \cdots, M, \\ & \sum_{m=1}^{M} r_l^m \ge \bar{r}_l,\ l = 1, \cdots, L, \\ & \mathbf{B}_l^m \mathrm{diag}(e^{\mathbf{r}^m})\mathbf{q}^m \le (\mathbf{I} + \mathbf{B}_l^m)\mathbf{q}^m, \\ & \qquad l = 1, \cdots, L;\ m = 1, \cdots, M, \\ \text{variables}:\quad & \mathbf{r}^m,\ m = 1, \cdots, M. \end{aligned} \tag{31}$$

Using the nonlinear Perron-Frobenius theorem [29] when Assumption 1 holds, we rewrite (31) into the following form:

$$\begin{aligned} \text{minimize}\quad & \sum_{m=1}^{M} \mathbf{1}^\top\left(\sum_{k=1}^{\infty}\left(\mathrm{diag}(e^{\mathbf{r}^m} - 1)\mathbf{F}^m\right)^k\right)(\mathbf{F}^m)^{-1}\mathbf{v}^m \\ \text{subject to}\quad & \log\rho\left(\widetilde{\mathbf{B}}_l^m \mathrm{diag}(e^{\mathbf{r}^m})\right) \le 0, \\ & \qquad l = 1, \cdots, L;\ m = 1, \cdots, M, \\ & \mathbf{r}^m \ge \mathbf{0},\ m = 1, \cdots, M, \\ & \sum_{m=1}^{M} r_l^m \ge \bar{r}_l,\ l = 1, \cdots, L, \\ \text{variables}:\quad & \mathbf{r}^m,\ m = 1, \cdots, M, \end{aligned} \tag{32}$$

because the last constraint in (31) is turned into:

$$\begin{aligned} &\mathbf{B}_l^m \mathrm{diag}(e^{\mathbf{r}^m})\mathbf{q}^m \le (\mathbf{I} + \mathbf{B}_l^m)\mathbf{q}^m \\ \Rightarrow\ &\rho\left(\widetilde{\mathbf{B}}_l^m \mathrm{diag}(e^{\mathbf{r}^m})\right) \le 1, \end{aligned} \tag{33}$$

which is a convex constraint.

Now, (32) is still non-convex solely because of the non-convex objective function. Assuming that each user transmits at a relatively high rate in each channel, $e^{r_l^m} - 1$ can be approximated as $e^{r_l^m}$ which is much larger than one for all l and m. It is different from (8) because the approximation

This article has been accepted for publication in a future issue of this journal, but has not been fully edited. Content may change prior to final publication. Citation information: DOI 10.1109/JIOT.2018.2792300, IEEE Internet of Things Journal

in objective function is only part of the non-convexity in (8). Then, (32) is approximated by:

$$\begin{aligned} \text{minimize} \quad & \sum_{m=1}^{M} \mathbf{1}^\top \left(\sum_{k=1}^{\infty} \left(\mathrm{diag}(e^{\mathbf{r}^m}) \mathbf{F}^m \right)^k \right) (\mathbf{F}^m)^{-1} \mathbf{v}^m \\ \text{subject to} \quad & \mathbf{r}^m \geq \mathbf{0}, \ m = 1, \cdots, M, \\ & \log \rho \left(\widetilde{\mathbf{B}}_l^m \mathrm{diag}(e^{\mathbf{r}^m}) \right) \leq 0, \\ & \quad l = 1, \cdots, L; \ m = 1, \cdots, M, \\ & \sum_{m=1}^{M} r_l^m \geq \bar{r}_l, \ l = 1, \cdots, L, \\ \text{variables :} \quad & \mathbf{r}^m, \ m = 1, \cdots, M. \end{aligned} \tag{34}$$

Note that (34) has a convex constraint set whenever Assumption 1 holds. However, we cannot guarantee that this assumption is always established.

B. General Convex Approximation

We convexify (22) by expanding the objective of (34) as the following approximation:

$$f^m(\mathbf{r}^m) = \left(e^{\mathbf{r}^m} \right)^\top \mathbf{F}^m \mathrm{diag}(\mathbf{v}^m) e^{\mathbf{r}^m} + (\mathbf{v}^m)^\top e^{\mathbf{r}^m}, \tag{35}$$

as $\mathbf{1}^\top \mathrm{diag}(\mathbf{x}) = \mathbf{x}^\top$ and $\mathrm{diag}(\mathbf{x})\mathbf{v} = \mathrm{diag}(\mathbf{v})\mathbf{x}$.

Without Assumption 1, we introduce the following nonnegative matrix by referring to [19]:

$$\widehat{\mathbf{B}}_l^m = (\mathbf{I} + \mathbf{B}_l^m + \mathrm{diag}(\boldsymbol{\epsilon}))^{-1} \left(\mathbf{B}_l^m - (\widetilde{\mathbf{X}}_l^m)^\star \right) \geq 0. \tag{36}$$

$(\widetilde{\mathbf{X}}_l^m)^\star$ is the optimal solution obtained by solving the following optimization problem:

$$\begin{aligned} \text{minimize} \quad & \|\widetilde{\mathbf{X}}_l^m\|_{\mathbf{F}} \\ \text{subject to} \quad & (\mathbf{I} + \mathbf{B}_l^m + \mathrm{diag}(\boldsymbol{\epsilon}))^{-1} \left(\mathbf{B}_l^m - (\widetilde{\mathbf{X}}_l^m)^\star \right) \geq 0, \\ & \widetilde{\mathbf{X}}_l^m \geq 0, \\ \text{variables :} \quad & \widetilde{\mathbf{X}}_l^m, \end{aligned} \tag{37}$$

where $\|\cdot\|_{\mathbf{F}}$ represents the Perron-Frobenius norm of a matrix. If $(\mathbf{I} + \mathbf{B}_l^m)$ is not invertible, $\boldsymbol{\epsilon}$ is a vector with each entry being a given small positive scalar, otherwise, ϵ can be an all zeros vector. (37) is a convex optimization problem which can be directly solved using numerical interior-point solvers, e.g., the CVX software [24]. Moreover, $(\widetilde{\mathbf{X}}_l^m)^\star$ is the all zeros matrix, if $\widetilde{\mathbf{B}}_l^m$ is nonnegative, i.e., the quasi-inverse of $(\widetilde{\mathbf{B}}_l^m)$ exists and $\widehat{\mathbf{B}}_l^m = \widetilde{\mathbf{B}}_l^m$. Otherwise, $(\widetilde{\mathbf{X}}_l^m)^\star$ is a relatively small matrix with most of its entries being zeros as compared to $\widetilde{\mathbf{B}}_l^m$.

We replace $\mathbf{B}_l^m$ on the left hand-side of the last constraint in (31) with $\mathbf{B}_l^m - (\widetilde{\mathbf{X}}_l^m)^\star$:

$$(\mathbf{B}_l^m - (\widetilde{\mathbf{X}}_l^m)^\star) \mathrm{diag}(e^{\mathbf{r}^m}) \mathbf{q}^m \leq (\mathbf{I} + \mathbf{B}_l^m) \mathbf{q}^m, \tag{38}$$

Then, we have:

$$\widehat{\mathbf{B}}_l^m \mathrm{diag}(e^{\mathbf{r}^m}) \mathbf{q}^m \leq \mathbf{q}^m. \tag{39}$$

By the use of the nonlinear Perron-Frobenius theorem [29], we approximate (3) to the following convex optimization problem finally:

$$\begin{aligned} \text{minimize} \quad & \sum_{m=1}^{M} \left(e^{\mathbf{r}^m} \right)^\top \mathbf{F}^m \mathrm{diag}(\mathbf{v}^m) e^{\mathbf{r}^m} + (\mathbf{v}^m)^\top e^{\mathbf{r}^m} \\ \text{subject to} \quad & \mathbf{r}^m \geq \mathbf{0}, \ m = 1, \cdots, M, \\ & \sum_{m=1}^{M} r_l^m \geq \bar{r}_l, \ l = 1, \cdots, L, \\ & \log \rho \left(\widehat{\mathbf{B}}_l^m \mathrm{diag}(e^{\mathbf{r}^m}) \right) \leq 0, \\ & \quad l = 1, \cdots, L; \ m = 1, \cdots, M, \\ \text{variables :} \quad & \mathbf{r}^m, \ m = 1, \cdots, M. \end{aligned} \tag{40}$$

In summary, we convexify the original non-convex problem (3) into a convex problem (40) related with the spectral radius constraints, by leveraging the nonnegative matrix theory and the approximation technique in [19]. Hence, we provide the following algorithm to approximate (3).

Algorithm 1 Efficient Convex Approximation Algorithm.

Require:
M: the number of channels.
L: the number of users.
G: the channel gain.
σ: the noise power.

if $\widetilde{\mathbf{B}}_l^m \geq 0$ **then**
- Replace $\widehat{\mathbf{B}}_l^m$ with $\widetilde{\mathbf{B}}_l^m$ to tackle (40).
- Get the corresponding optimal value $(\mathbf{r}^m)^\star$.

else
- Tackle (37) to obtain $(\widetilde{\mathbf{X}}_l^m)^\star$.
- Computer $\widehat{\mathbf{B}}_l^m$ by (36).
- Solve (40) to obtain the value $(\mathbf{r}^m)^\star$.

end if
Obtain the approximation solution $\mathbf{p}^m$ from (11).

Remark 1. *The convex approximation* $\rho\left(\widehat{\mathbf{B}}_l^m \mathrm{diag}(e^{\mathbf{r}^m})\right)$ *is tight indeed, if the corresponding quasi-inverse condition holds [19].* $\log \rho\left(\widehat{\mathbf{B}}_l^m \mathrm{diag}(e^{\mathbf{r}^m})\right)$ *is a convex function in terms of* $\mathbf{r}^m$ *for the irreducible nonnegative matrix* $\widehat{\mathbf{B}}_l^m$*, because of the log-convexity property of the nonlinear Perron-Frobenius eigenvalue [30]. Therefore,* (40) *is a convex optimization problem indicating that we can tackle* (3) *in polynomial time, which is the corresponding upper bound of* (3).

The upper bound computed by Algorithm 1 motivates us to study its lower bound so that we eventually obtain the global optimal value of (3). Next, we leverage the convex relaxation technique to get the lower bound of (3), and desgin the global optimization algorithm via the branch-and-bound framework [27].

V. Global Optimization Algorithm

In this section, we work on exploiting the lower bound and the branch-and-bound method to obtain the global optimal value of (3) by iteratively making the convex relaxation.

This article has been accepted for publication in a future issue of this journal, but has not been fully edited. Content may change prior to final publication. Citation information: DOI 10.1109/JIOT.2018.2792300, IEEE Internet of Things Journal

Letting p_l^m = $e^{\tilde{p}_l^m}$ and taking the log function on the outage constraint, we change (7) into the following equivalent optimization problem:

$$\begin{aligned} \text{minimize} \quad & \sum_{l=1}^{L}\sum_{m=1}^{M} e^{\tilde{p}_l^m} \\ \text{subject to} \quad & \log \mathsf{SINR}_l^m(e^{\tilde{\mathbf{p}}^m}) \geq \log(e^{r_l^m}-1), \\ & \quad l=1,\cdots,L;\ m=1,\cdots,M, \\ & \sum_{m=1}^{M} r_l^m \geq \bar{r}_l,\ l=1,\cdots,L, \\ & e^{\tilde{p}_l^m} \leq \bar{p}_l^m,\ l=1,\cdots,L;\ m=1,\cdots,M, \\ & \mathbf{r}^m \geq \mathbf{0},\ m=1,\cdots,M, \\ \text{variables :} \quad & \tilde{\mathbf{p}}^m,\ \mathbf{r}^m,\ m=1,\cdots,M. \end{aligned} \tag{41}$$

Note that $\log \mathsf{SINR}_l^m(e^{\tilde{\mathbf{p}}^m})$ is a concave function with respect to $\tilde{\mathbf{p}}^m$, and the main non-convexity is solely caused by $\log(e^{r_l^m}-1)$ in (41). Therefore, we relax the function $\log(e^{r_l^m}-1)$ in the rate constraints over the box set $\Big\{r_l^m \mid \epsilon \leq r_l^m \leq \min\big\{\log(1+\bar{p}_l^m/v_l^m),\ \bar{r}_l^m\big\}\Big\}$ for all m and l, where ϵ is a small enough positive value to approximate zero, i.e., $\epsilon \to 0$. In other words, we consider the initial box set as $\mathcal{Q}_{init}$ = $\Big\{r_l^m \mid \epsilon \leq r_l^m \leq \min\big\{\log(1+\bar{p}_l^m/v_l^m),\ \bar{r}_l^m,\big\}\Big\}$, to get the following convex optimization problem:

$$\begin{aligned} \text{minimize} \quad & \sum_{l=1}^{L}\sum_{m=1}^{M} e^{\tilde{p}_l^m} \\ \text{subject to} \quad & \log(e^{\bar{r}_l}-1) + \frac{\log(e^{\bar{r}_l}-1)-\log(e^{\epsilon}-1)}{\bar{r}_l-\epsilon} \\ & \times(r_l^m-\bar{r}_l) - \log \mathsf{SINR}_l^m(e^{\tilde{\mathbf{p}}^m}) \leq 0, \\ & \quad l=1,\cdots,L;\ m=1,\cdots,M, \\ & \sum_{m=1}^{M} r_l^m \geq \bar{r}_l,\ l=1,\cdots,L, \\ & e^{\tilde{p}_l^m} \leq \bar{p}_l^m,\ l=1,\cdots,L;\ m=1,\cdots,M, \\ & \mathbf{r}^m \geq \mathbf{0},\ m=1,\cdots,M, \\ \text{variables :} \quad & \tilde{\mathbf{p}}^m,\ \mathbf{r}^m,\ m=1,\cdots,M. \end{aligned} \tag{42}$$

Notably, (42) is convex indicating that we can numerically solve it, e.g., the interior-point solvers in the cvx software [24]. Then, the box constraints are iteratively subdivided to smaller subsets for the exhaustive searching, based on the lower bound and the upper bound of (3) using the branch-and-bound framework. The exhaustive searching is organized as a binary tree, in which the leaf nodes represent the union of the sets. At each leaf node, we get the corresponding upper bound and lower bound to (3).

Given the box constraint set $[b_l^m, u_l^m]$ of individual rate r_l^m for all l and m, the upper bound for (3) is provided by Algorithm 1 and the lower bound is obtained by solving (42). Thus, we get the global optimal value of (3) by proposing the following global optimization algorithm, which takes Algorithm 1 as the submodule and leveraging the relaxation technique above.

For clarity, let k stand for the iteration index and $\mathcal{L}_k$ denote the set of rectangles. The functions Φ_{ub} and Φ_{lb} compute the upper and lower bounds, respectively.

Algorithm 2 Global Optimal Algorithm.

1) **Initialization**
   - Let $\mathcal{Q}_{init}$ be the initial rectangular set $[b_l^m, u_l^m]$ for $m \in \mathcal{M}$ and $l \in \mathcal{L}$. In addition, $k=0$ and $\mathcal{Q}_0 = \{\mathcal{Q}_{init}\}$. Besides, $b_l^m = \epsilon$ and $u_l^m = \min\{\log(1+\bar{p}_l^m/v_l^m),\ \bar{v}_l^m\}$.
   - Obtain the lower bound $L_0 = \Phi_{lb}(\mathcal{Q}_{init})$ for (3) by obtaining the following optimal value of the convex optimization problem:

$$\begin{aligned} \text{minimize} \quad & \sum_{l=1}^{L}\sum_{m=1}^{M} e^{\tilde{p}_l^m} \\ \text{subject to} \quad & \log(e^{u_l^m}-1) + \\ & \frac{\log(e^{u_l^m}-1)-\log(e^{b_l^m}-1)}{u_l^m-b_l^m} \\ & \times(r_l^m-u_l^m) - \log \mathsf{SINR}_l^m(e^{\tilde{\mathbf{p}}^m}) \leq 0, \\ & \quad l=1,\cdots,L;\ m=1,\cdots,M, \\ & \sum_{m=1}^{M} r_l^m \geq \bar{r}_l,\ l=1,\cdots,L, \\ & e^{\tilde{p}_l^m} \leq \bar{p}_l^m,\ l=1,\cdots,L;\ m=1,\cdots,M, \\ & \mathbf{r}^m \geq \mathbf{0},\ m=1,\cdots,M, \\ \text{variables :} \quad & \tilde{\mathbf{p}}^m,\ \mathbf{r}^m,\ m=1,\cdots,M. \end{aligned} \tag{43}$$

   - Compute the upper bound $U_0 = \Phi_{ub}(\mathcal{Q}_{init})$ for (3) by running Algorithm 1.
2) **Convergence Criterion**
   - Stop iteration if U_k - $L_k < \epsilon$.
   - Go to next step, otherwise.
3) **Branching**
   - Choose a rectangular set $\mathcal{Q} \in \mathcal{L}_k$ s.t. $\Phi_{lb}(\mathcal{Q}) = L_k$.
   - Split the rectangle $\mathcal{Q}$ along its longest edges into the new rectangles $\mathcal{Q}_I$ and $\mathcal{Q}_{II}$.
   - Update $\mathcal{L}_{k+1} \triangleq (\mathcal{L}_k - \{Q\}) \cup \{\mathcal{Q}_I,\ \mathcal{Q}_{II}\}$.
   - Update $L_{k+1} \triangleq \min_{\mathcal{Q}\in L_{k+1}} \Phi_{lb}(\mathcal{Q})$.
   - Update $U_{k+1} \triangleq \min_{\mathcal{Q}\in L_{k+1}} \Phi_{ub}(\mathcal{Q})$.
4) **Pruning**
   - Remove all rectangles $\mathcal{Q}$ from $\mathcal{L}_{k+1}$ if $\Phi_{lb}(\mathcal{Q}) > U_{k+1}$.
   - Update $k \leftarrow k+1$ and go to Step 2.

Theorem 3. *Algorithm 2 must converge to the global optimal value of* (3) *from any initial rectangular* $\mathcal{Q}_{init}$.

Proof: We tackle the convex relaxation problem (43) to obtain the lower bound of (3), and obtain the upper bound by running Algorithm 1. Algorithm 2 is guaranteed to terminate in finite number of steps based on the lower and upper bounds [27]. ∎

This article has been accepted for publication in a future issue of this journal, but has not been fully edited. Content may change prior to final publication. Citation information: DOI 10.1109/JIOT.2018.2792300, IEEE Internet of Things Journal

Remark 2. *We get the upper bound for* (3) *by taking Algorithm 1 as the inner loop at Step 1 of Algorithm 2. L_k consists of all the leaves representing the child nodes in a binary tree. Steps 3 and 4 in Algorithm 2, i.e., namely "Branching" and "Pruning", are searching the global lower bound for the optimal value of* (3)*. If $b_l^m = 0$ for some l and m, let $b_l^m = \epsilon$ where ϵ approximates zero which is a small enough positive value, i.e., $\epsilon \to 0$.*

Remark 3. *In Step 3 "Branching", we split the picked rectangle along one of its longest edges, which partitions the least number of the rectangles. It is obvious that unmanageably large number of rectangles may be partitioned with the increase of iterations. Therefore, we delete some rectangles that satisfy $\Phi_{lb}(\mathcal{Q}) > U_{k+1}$ by eliminating them from $\mathcal{L}_{k+1}$ in Step 4 "Pruning". They need not to be considered in the subsequent iterations so as to reduce the overall searching time of Algorithm 2, as the optimal value can not be found in these subsets.*

VI. Numerical Simulations

We evaluate the performance of the proposed algorithms numerically leveraging the CVX software package [24] in MATLAB R2014b in this section. Note that if $M = 1$, the original optimization problem can be reduced to the simple form under the commonly-known single-channel multi-user networks, where the users communicate by sharing the same frequency-fading channel. Moreover, it can be directly tackled via the distributed power control algorithm in [31]. When $M > 1$, it is noticed that the matrix $\mathbf{G}$ representing the channel gains changes to a M-dimensional matrix from a just two-dimensional matrix, consisted by a number of two-dimensional matrices.

We employ the model $G_{lj}^m = k^m(d_{lj})^{-\alpha^m}$ in [32] for the channel gain, where k^m is an attenuation factor representing the power variation because of the path loss, and α^m is a pass loss coefficient on the m-th channel. All of them depend on the practical environments. In usual, k^m depends on the horizontal layer between the wireless terminals and the base stations and the frequency of communications. In addition, d_{lj} represents the Euclidean distance from the j-th transmitter to the l-th receiver. We set $\alpha^m = 2$ for all m and $\mathbf{k}$ = [0.3, 0.5, 0.8] based on the empirical values.

In this example, we compare our proposed Algorithm 1 with the approximation value of (8) which is efficient for the high SINR environments in [23], the iterative power evolution algorithm in [33] and the global optimal value obtained by the branch-and-bound Algorithm 2. The budgets of the transmit power and the requirements of the data rate are set as the same for all users and channels, i.e., $\bar{p}_l^m = 1.5$ w and $\bar{r}_l = 0.6$ nats/symbol. The simulation results are demonstrated in Figure 4, where the blue solid line illustrates the evolution and convergence of the total power in [33], the red dotted line shows the approximate value obtained from Algorithm 1, the green dashed line shows the outcome of the approximate value solved by the convex optimization problem (8) and the purple dot-dash line represents the global optimal value of total power obtained by Algorithm 2. L and M are set as 2, 4, 6 and 2, 3,

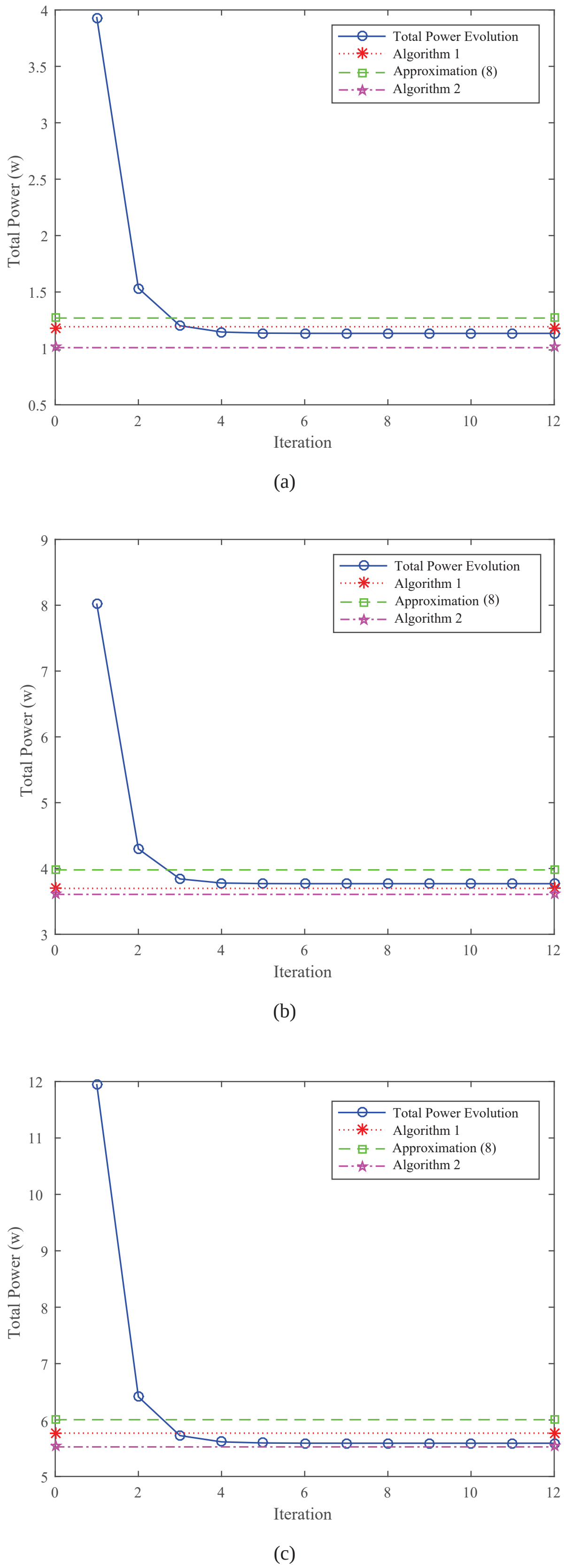

Fig. 4: Comparisons between Algorithm 1, iterative power evolution, the approximation (8) and Algorithm 2.

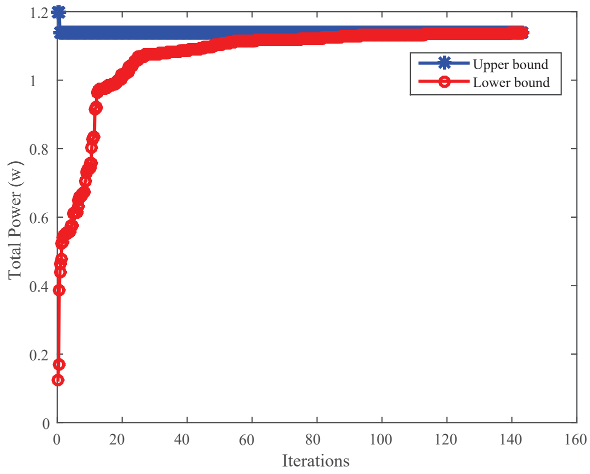

(a)

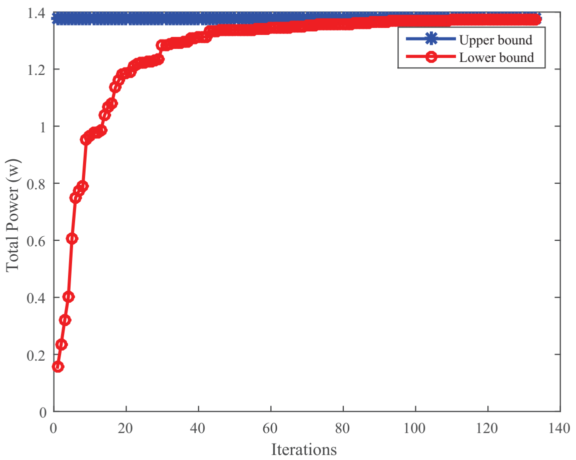

(b)

Fig. 5: Illustrations of the convergence of Algorithm 2.

5 in the subfigures, respectively. It is shown that the iterative power evolution algorithm converges fast to an equilibrium of (3). The approximation (8) approaches this equilibrium but with a small gap. Compared to the iterative power evolution algorithm, Algorithm 1 is insensitive to initialization. Algorithm 1 obtains a better approximate value as shown in Figure 4, when the iterative power evolution algorithm uses the bad initial point. Therefore, Algorithm 1 is more stable. Moreover, Algorithm 1 is better than the approximation (8) in practice, as the value of green line is somewhat higher than the value of red line.

Furthermore, the convergence of Algorithm 2 is plotted in Figure 5 for the two users communicating through two channels. The network parameters are the same as those in Figure 4, and we set $\epsilon = 0.001$. The evolutions of the lower bound and the upper bound of the optimization problem (3) are depicted by the red lines and blue lines, respectively. It is shown that Algorithm 2 converges at the 146-th iteration in Figure 5(a) and at the 137-th iteration in Figure 5(b). The approximation value computed from Algorithm 1 almost achieves the global optimal value in the first few iterations.

VII. Conclusion

In this paper, we formulated a total power minimization problem according to the Shannon capacity formula with power and SINR constraints. We convexified it by leveraging the nonnegative matrix theory to obtain a convex optimization problem with rate as the only variable. Thus, the total power minimization problem is polynomial time solvable to get an approximated value. Motivated by the upper bound of the approximation value, we obtained the lower bound by employing the convex relaxation technique. Leveraging the branch-and-bound framework, we took the convex approximation method as an inner loop to compute the global optimal value. Numerical simulations demonstrated that our proposed algorithms can achieve the efficient power and rate allocations.

Acknowledgements

The authors acknowledge helpful discussions with Prof. Chee Wei Tan, Dr. Feng Zhang and Dr. Liang Zheng. The authors also gratefully acknowledge helpful comments of the Editor and anonymous reviewers.

References

[1] E. Hossain and M. Hasan. 5G cellular: Key enabling technologies and research challenges. *IEEE Instrumentation & Measurement Magazine*, 18(3):11–21, 2015.

[2] C. Zhu, J. J. P. C. Rodrigues, V. C. M. Leung, L. Shu, and L. T. Yang. Trust-based communication for industrial internet of things. *IEEE Communications Magazine*, 2018.

[3] C. Zhu, V. C. M. Leung, L. Shu, and E. C.-H. Ngai. Green internet of things for smart world. *IEEE Access*, 3:2151–2162, Nov. 2015.

[4] A. Al-Fuqaha, M. Guizani, M. Mohammadi, M. Aledhari, and M. Ayyash. Internet of things: A survey on enabling technologies, protocols, and applications. *IEEE Communications Surveys & Tutorials*, 17(4):2347–2376, 2015.

[5] C. Zhu, L. Shu, V. C. M. Leung, S. Guo, Y. Zhang, and L. T. Yang. Secure multimedia big data in trust-assisted sensor-cloud for smart city. *IEEE Communications Magazine*, 55(12):24–30, Dec. 2017.

[6] F. Xiao, Z. Wang, N. Ye, R. Wang, and X.-Y. Li. One more tag enables fine-grained RFID localization and tracking. *IEEE/ACM Transactions on Networking*, pages 1–14, 2017.

[7] B. Chen, C. Zhu, W. Li, J. Wei, V. C. M. Leung, and L. T. Yang. Original symbol phase rotated secure transmission against powerful massive MIMO eavesdropper. *IEEE Access*, 4:3016–3025, 2016.

[8] C. Zhu, H. Zhou, V. C. M. Leung, K. Wang, Y. Zhang, and L. T. Yang. Toward big data in green city. *IEEE Communications Magazine*, 55(11):14–18, Nov. 2017.

[9] C. Zhu, V. C. M. Leung, K. Wang, L. T. Yang, and Y. Zhang. Multi-method data delivery for green sensor-cloud. *IEEE Communications Magazine*, 55(5):176–182, May 2017.

[10] X. Zhai, L. Zheng, and C. W. Tan. Energy-infeasibility tradeoff in cognitive radio networks: Price-driven spectrum access algorithms. *IEEE Journal on Selected Areas in Communications*, 32(3):528–538, Mar. 2014.

[11] X. Zhai, C. W. Tan, Y. Huang, and B. D. Rao. Transmit beamforming and power control for optimizing the outage probability fairness in miso networks. *IEEE Transactions on Communications*, 65(2):839–850, Feb. 2017.

[12] M. Moltafet, P. Azmi, and N. Mokari. Power minimization in 5G heterogeneous cellular networks. *Iranian Conference on Electrical Engineering*, pages 234–238, 2016.

[13] X. Sun and S. Wang. Resource allocation scheme for energy saving in heterogeneous networks. *IEEE Transactions on Wireless Communications*, 14(8):4407–4416, 2015.

[14] A. Ghazanfari, A. Tolli, and H. Pennanen. Sum power minimization for cellular systems with underlay D2D communications. In *International Conference on Cognitive Radio Oriented Wireless Networks and Communications*, pages 45–50, 2014.

[15] Y. Jiang, Q. Liu, F. Zheng, X. Gao, and X. You. Energy efficient joint resource allocation and power control for D2D communications. *IEEE Transactions on Vehicular Technology*, 65(8):6119–6127, 2016.

[16] L. Zhou, C. Zhu, R. Ruby, X. Wang, X. Ji, S. Wang, and J. Wei. QoS-aware energy-efficient resource allocation in OFDM-based heterogenous cellular networks. *International Journal of Communication Systems*, 30(2), 2015.

[17] Y. Li, M. Sheng, X. Wang, and Y. Shi. Globally optimal antenna selection and power allocation for energy efficiency maximization in downlink distributed antenna systems. In *Global Communications Conference*, pages 3856–3861, 2014.

[18] Y. C. Zhao, J. Wu, W. Z. Li, and S. L. Lu. Throughput optimization in cognitive radio networks ensembling physical layer measurement. *Journal of Computer Science and Technology*, 30(6):1290–1305, 2015.

[19] L. Zheng and C. W. Tan. Maximizing sum rates in cognitive radio networks: Convex relaxation and global optimization algorithms. *IEEE Journal on Selected Areas in Communications*, 32(3):667–680, 2014.

[20] S. Ren and V. D. S. Mihaela. Distributed power allocation in multi-user multi-channel cellular relay networks. *IEEE Transactions on Wireless Communications*, 9(6):1952–1964, 2010.

[21] S. Li, Z. Zheng, E. Ekici, and N. Shroff. Maximizing system throughput using cooperative sensing in multi-channel cognitive radio networks. *IEEE Conference on Decision and Control*, 22(4):5858–5863, 2012.

[22] X. Guan, X. Zhai, C. Zhu, and J. Yuan. Total power minimization for high rate communication in multi-channel multi-user wireless networks. *IEEE International Conference on High Performance Computing and Communications*, pages 824–830, 2016.

[23] M. Chiang. Balancing transport and physical layers in wireless multi-hop networks: Jointly optimal congestion control and power control. *IEEE/ACM Transactions on Communications*, 23(1):104–116, Jan. 2005.

[24] M. Grant and S. Boyd. CVX: Matlab software for disciplined convex programming, 2008.

[25] J. S. Pang, G. Scutari, D. P. Palomar, and F. Facchinei. Design of cognitive radio systems under temperature-interference constraints: A variational inequality approach. *IEEE Transactions on Signal Processing*, 58(6):2994–2997, 2010.

[26] E. Seneta. *Non-Negative Matrices and Markov Chains*. Springer Science & Business Media, 2006.

[27] S. Boyd and L. Vandenberghe. *Convex Optimization*. Cambridge University Press, 2004.

[28] C. W. Tan, S. Friedland, and S. Low. Nonnegative matrix inequalities and their application to nonconvex power control optimization. *SIAM Journal on Matrix Analysis and Applications*, 32(3):1030–1055, 2011.

[29] S. Friedland and S. Karlin. Some inequalities for the spectral radius of non-negative matrices and applications. *Duke Mathematical Journal*, 42(3):459–490, 1975.

[30] U. Krause. Concave Perron-Frobenius theory and applications. *Nonlinear Analysis: Theory, Methods & Applications*, 47(3):1457–1466, 2001.

[31] G. J. Foschini and Z. Miljanic. A simple distributed autonomous power control algorithm and its convergence. *IEEE Transactions on Vehicular Technology*, 42(4):641–646, 1993.

[32] J. D. Parsons. *The Mobile Radio Propagation Channel*. John Wiley, 2007.

[33] J. D. Matyjas, S. Kumar, and F. Hu. Spectrum sharing in wireless networks: Fairness, efficiency, and security. *CRC Press*, 2016.

Xiangping (Bryce) Zhai (M'15) received the B.Eng. degree in Computer Science and Technology from Shandong University in 2006, and the Ph.D. degree in Computer Science from City University of Hong Kong in 2013. Previously, he was a Postdoctoral Fellow at the City University of Hong Kong. He is currently an Assistant Professor of the College of Computer Science and Technology, Nanjing University of Aeronautics and Astronautics, China. His research interests are in the area of Internet of Things, power control, edge computing, resource optimization and spatial analytics. He has been actively involved in organizing and chairing sessions, and has served as reviewer for several journals and TPC for several international conferences.

Xiaoxiao Guan received the B.E. degree in computer science and technology from the Department of Computer and Control Engineering, Yantai University, Yantai, China, in 2015. She is pursuing her M.S. degree at the Nanjing University of Aeronautics and Astronautics. Her research interests are in wireless networks and nonlinear optimization.

Chunsheng Zhu received the Ph.D. Degree in Electrical and Computer Engineering from The University of British Columbia, Canada. He is currently a Postdoctoral Research Fellow in the Department of Electrical and Computer Engineering at The University of British Columbia in Canada. He has authored more than 100 publications published by refereed international journals (e.g., IEEE Transactions on Industrial Electronics, IEEE Transactions on Computers, IEEE Transactions on Information Forensics and Security, IEEE Transactions on Industrial Informatics, IEEE Transactions on Vehicular Technology, IEEE Transactions on Emerging Topics in Computing, IEEE Transactions on Cloud Computing, ACM Transactions on Embedded Computing Systems, ACM Transactions on Cyber-Physical Systems), magazines (e.g., IEEE Communications Magazine, IEEE Wireless Communications Magazine, IEEE Network Magazine), and conferences (e.g., IEEE INFOCOM, IEEE IECON, IEEE SECON, IEEE DCOSS, IEEE ICC, IEEE GLOBECOM). His research interests mainly include Internet of Things, wireless sensor networks, cloud computing, big data, social networks, and security.

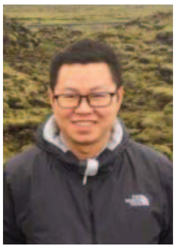

Lei Shu (SM'16) is a Lincoln Professor with the University of Lincoln, UK, and a distinguished professor with Nanjing Agricultural University, China. He is also the director of the NAU-Lincoln Joint Research Center of Intelligent Engineering. His main research field is wireless sensor networks. He has authored over 360 papers in related conferences, journals, and books in the area of sensor networks. He was awarded the GlobeCom 2010 and the ICC 2013 Best Paper Award, IEEE Systems Journal 2017 Best Paper Award. He has served as a TPC member for over 150 conferences, such as ICDCS, DCOSS, MASS, ICC, GlobeCom, ICCCN, WCNC, and ISCC. He has also served as cochair for more than 50 international conferences and workshops, such as IWCMC, ICC, ISCC, ICNC, and Chinacom, as well as symposium cochair for IWCMC 2012 and ICC 2012, general cochair for Chinacom 2014, Qshine 2015, CollaborateCom 2017, and Mobiquitous 2018, and as steering and the TPC chair for InisCom 2015. He has been serving as an associate editor for IEEE Transactions on Industrial Informatics, IEEE Communications Magazine, IEEE Systems Journal and IEEE Access.

Jiabin Yuan received the Ph.D. degree in Testing Technology and Instrumentation from the Department of Automation, Nanjing University of Aeronautics and Astronautics, Nanjing, China, 2000. He is a Professor with the Department of Computer Science and Technology, Nanjing University of Aeronautics and Astronautics, Nanjing, China. His research interests include Cryptology, Computer Networks and Security, Grid and Cloud Computing, and Internet of Things.